Supplementary Material:
k-space optical microscopy of nanoparticle arrays: opportunities and artifacts

Jean-François Bryche,[1,2] Grégory Barbillon,[1,3] Bernard Bartenlian,[1] Gérald Dujardin,[4] Elizabeth Boer-Duchemin,[4] and Eric Le Moal[4,a)]

[1)] *Centre de Nanosciences et de Nanotechnologies, CNRS, Univ. Paris-Sud, Université Paris-Saclay, C2N - Orsay, 91405 Orsay cedex, France*

[2)] *Laboratoire Charles Fabry, CNRS, Institut d'Optique Graduate School, Université Paris-Saclay, 2 Avenue Augustin Fresnel, 91127 Palaiseau Cedex, France*

[3)] *EPF-Ecole d'Ingénieurs, 3 bis rue Lakanal, 92330 Sceaux, France*

[4)] *Institut des Sciences Moléculaires d'Orsay (ISMO), CNRS, Univ Paris Sud, Université Paris-Saclay, 91405 Orsay Cedex, France*

(Dated: June 29, 2018)

In this Supplementary Material, aditional experimental details and an additional discussion of the interpretation of Fourier-space images can be found. Moreover, the effect of the objective properties on the "condenser effect" (which is due to spurious reflections in the objective) is examined.

ADDITIONAL EXPERIMENTAL DETAILS

Figure S1 shows schematically an additional illumination configuration used in this study. Similarly to the configurations shown in Figs. 1(a) and 1(b) in the article, the initial illumination is through the transparent substrate, and the objective lens is used for both the illumination of the sample and for the collection of the light that is reflected or back scattered (*episcopic* configuration). The initial light beam from a CW linearly polarized He-Ne laser (vacuum wavelength λ_0 = 632.8 nm) is collimated, with variable angles of incidence ($\theta_{inc} > 0°$). This configuration is similar to a Surface Plasmon Resonance (SPR) system[S1], where the internal interface of a metal-coated glass slide is illuminated with a collimated light beam and the intensity of the reflected light is measured as a function of the polar angle of incidence. An intensity minimum is expected at an angle where the incident light resonantly couples to surface plasmon polaritons (SPPs) at the external interface of the metallic layer. The SPP wavevector may be determined from the angular position of this dip in intensity. Here, in an adaptation of this technique we not only monitor the intensity of the reflected beam but also that of the light back-scattered at other angles from the periodic array, leading to a complementary method for measuring the SPP wavevector.

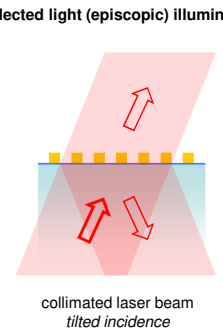

Figure S1. Schematics of an additional illumination configuration used in this study. The sample is illuminated through the substrate with a collimated laser beam of variable angle of incidence and the reflected and back-scattered light is collected in reflection using the same objective lens.

ADDITIONAL DISCUSSION OF THE INTERPRETATION OF FOURIER-SPACE IMAGES

In Sec. IIIA in the article, we describe an effect that is responsible for the occurrence of narrow rings at a radius slightly below the numerical aperture of the objective (NA=1.49 in the present case) in certain Fourier-space images. These Fourier-space images are of nanodot arrays on transparent or semi-transparent substrates and have been obtained in a reflected light illumination configuration with a focused laser beam. This first effect is due to a well-known optical phenomenon where light undergoes a phase shift upon total internal reflection at a dielectric-dielectric interface[S2,S3]. A second effect, occurring inside the microscope objective, may further shift the phase of the reflected and diffracted light at supercritical angles, depending on the type of microscope objective used. The evanescent field of an emitter in a dielectric medium and close ($< \lambda$) to a second dielectric of higher index of refraction can couple to the photonic (or propagating) modes of the second medium. The resulting emission of light at supercritical angles is known to be phase shifted to compensate for the phase mismatch between the resulting waves in the two different media of different indices of refraction (see Ref. S4 on p.353). This shift increases with emission angle. In principle, this effect should not play a role in the present study, since we are measuring the emission that is totally internally reflected and not molecular (dipole) emission; however, the

[a)] eric.le-moal@u-spud.fr

optics of high-NA, oil-immersion, microscope objectives are specifically corrected for this effect, when they are designed for total-internal-reflection fluorescence (TIRF) microscopy, in order to restore the optimal point spread function of the microscope. The phase shift is compensated by introducing a phase delay that is dependent on the polar angle. In the illumination configuration used here, the light beam wavefront is thus modified twice (when going in and then out of the objective after reflection). This is expected to increase the total phase shift undergone by light upon total internal reflection.

Now, we discuss the **x**/**y** asymmetry of the Fourier-space images of the nanodot array shown in Fig. 3 in the article, which is more pronounced than that of the structureless area shown in Fig. 3(d). The intensity is higher along the **x** axis, as is clearly visible in the intensity ratio shown in Fig. 3(e). This is due to the fact that the relative amplitude and phase of the scattered light beams from the periodic array depend on the (i, j) diffraction orders considered and the incident light polarization. The intensity pattern seen in Fig. 3(c) is indeed rotated by 90° when the polarization is changed from $\mathbf{E_{inc}} \parallel \mathbf{y}$ to $\mathbf{E_{inc}} \parallel \mathbf{x}$.

EFFECT OF THE OBJECTIVE PROPERTIES ON THE "CONDENSER EFFECT"

Finally, we examine the effect of the objective properties on the "condenser effect", with the aim of showing that this artifact is not specific to a particular microscope objective. Figure S2(a) shows a picture of two high-NA, oil-immersion, microscope objectives. On the right is the Nikon 100× 1.49 NA objective used for all the experiments reported in the article and the supplemental material, with the exception of the present Section. On the left is a different objective from another company (an Olympus PlanApoN TIRF objective), which differs in magnification factor (60×) and NA (1.45). Moreover, the front lens of the Olympus objective is held by a dark casing, presumably to prevent reflection issues, in contrast to the shiny metallic casing of the Nikon objective. To investigate whether changing these parameters has an impact on the "condenser effect", we carry out once again the same experiments as those performed in Figs. 4(b) and 4(c) in the article, but this time using the Olympus 60× 1.45 NA objective. In practice, the Olympus objective is mounted on the Nikon revolving noisepiece using a 15 mm length expander and an RMS-to-M25 thread adapter (Olympus and Nikon objectives have different parfocal distances and thread types).

The resulting Fourier-space images are shown in Figs. S2(b) and S2(c) and intensity profiles taken from the image on the right are shown in Fig. S2(d). The same artifacts as observed with the Nikon objective may be seen. Both the geometry of the features observed in Figs. S2(b) and S2(c) and their relative intensity compared to the $(0, 0)$ spot are similar to those measured in Figs. 4(b) and 4(c), respectively. In particular, whatever the external aspect (dark vs. shiny) of the casing that holds the front lens, the intensity of the off-centered rings due to the "condenser effect" is about 0.1% of that of the $(0, 0)$ spot. However, the radius of the rings is smaller than in Fig. 4, presumably due to the lower NA of the Olympus objective. Moreover, a disk is again seen in the middle of the Fourier-space image. The radius of this disk is $k_{\parallel}/k_0 = 0.83$ (i.e., 33°).

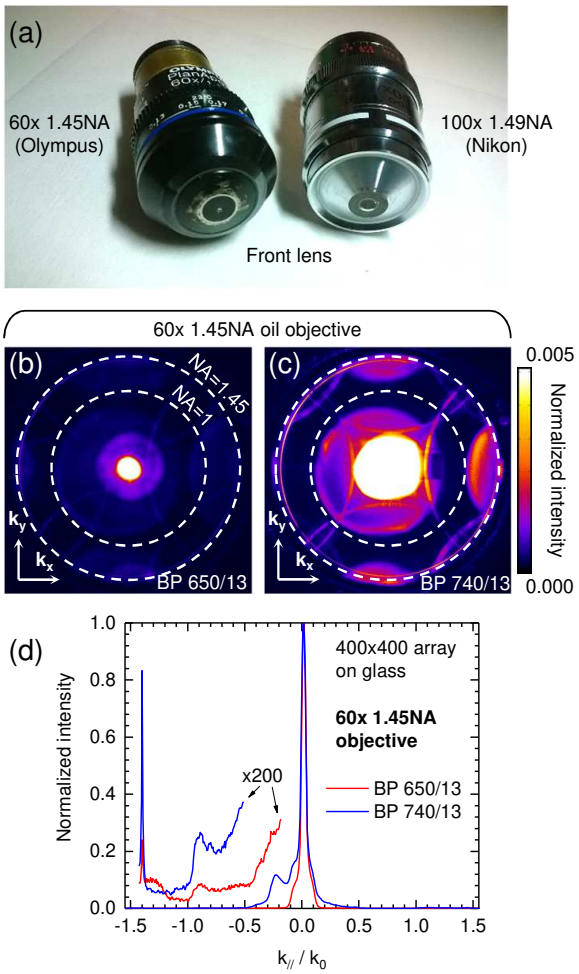

Figure S2. (a) Picture of an Olympus 60× 1.45 NA oil objective on the left and a Nikon 100× 1.49 NA oil objective on the right. This Nikon objective is used in all the other experiments discussed in the article. [(a) and (b)] Fourier-space optical microscopy images of a 400 × 400 nm periodic gold nanodot array on bare glass measured with the Olympus 60× 1.45 NA oil objective shown in (a). All images are obtained in a transmitted light illumination configuration using a collimated white light beam with normal incidence, as shown in Fig. 2(c). Bandpass filters with a 13 nm bandwidth centered on a wavelength of 650 nm is used in (b) and 740 nm in (c), respectively. The intensity scale shown on the right is normalized with respect to the $(0, 0)$ spot intensity. (d) Intensity profiles taken from the image shown in (c) along the $\mathbf{k_x}$-axis.

ACKNOWLEDGMENTS

We acknowledge technical support from the micro-nanotechnology platform of the Center for Nanosciences and Nanotechnologies (C2N-CTU) in Orsay, France, and financial support from the Région Ile-de-France in the framework of DIM Nano-K. We thank Dr S. Lévêque-Fort for enlightning discussions and the loan of the Olympus objective.

REFERENCES

[S1]J. Homola, S. S. Yee, and G. Gauglitz, "Surface plasmon resonance sensors: review," Sens. Actuator B-Chem. **54**, 3 – 15 (1999).

[S2]R. M. A. Azzam, "Phase shifts that accompany total internal reflection at a dielectric - dielectric interface," J. Opt. Soc. Am. A **21**, 1559–1563 (2004).

[S3]R. M. A. Azzam, "Phase shifts in frustrated total internal reflection and optical tunneling by an embedded low-index thin film," J. Opt. Soc. Am. A **23**, 960–965 (2006).

[S4]L. Novotny and B. Hecht, *Principles of Nano-Optics* (Cambridge University Press, 2006) DOI: 10.1017/CBO9780511813535.